

## THE RELATION BETWEEN BLACK HOLE MASS, BULGE MASS, AND NEAR-INFRARED LUMINOSITY

ALESSANDRO MARCONI<sup>1</sup> AND LESLIE K. HUNT<sup>2</sup>

Received 2003 March 6; accepted 2003 April 14; published 2003 April 18

### ABSTRACT

We present new accurate near-infrared (NIR) spheroid (bulge) structural parameters obtained by a two-dimensional image analysis of all galaxies with a direct black hole (BH) mass determination. As expected, NIR bulge luminosities  $L_{\text{bul}}$  and BH masses are tightly correlated, and if we consider only those galaxies with a secure BH mass measurement and an accurate  $L_{\text{bul}}$  (27 objects), the spread of  $M_{\text{BH}}-L_{\text{bul}}$  is similar to  $M_{\text{BH}}-\sigma_e$ , where  $\sigma_e$  is the effective stellar velocity dispersion. We find an intrinsic rms scatter of  $\approx 0.3$  dex in  $\log M_{\text{BH}}$ . By combining the bulge effective radii  $R_e$  measured in our analysis with  $\sigma_e$ , we find a tight linear correlation (rms  $\approx 0.25$  dex) between  $M_{\text{BH}}$  and the virial bulge mass ( $\propto R_e \sigma_e^2$ ), with  $\langle M_{\text{BH}}/M_{\text{bul}} \rangle \sim 0.002$ . A partial correlation analysis shows that  $M_{\text{BH}}$  depends on both  $\sigma_e$  and  $R_e$  and that both variables are necessary to drive the correlations between  $M_{\text{BH}}$  and other bulge properties.

*Subject headings:* black hole physics — galaxies: bulges — galaxies: fundamental parameters — galaxies: nuclei

### 1. INTRODUCTION

Central massive black holes (BHs) are now thought to reside in virtually all galaxies with a hot spheroidal stellar component (hereafter bulge). Such BHs seem to be a relic of past quasar activity (e.g., Softan 1982; Marconi & Salvati 2002; Yu & Tremaine 2002; Aller & Richstone 2002) and related to host galaxy properties, with the implication that BH and galaxy formation processes are closely linked. Previous work has shown that BH mass  $M_{\text{BH}}$  is correlated with both blue luminosity  $L_{B, \text{bul}}$  and bulge mass  $M_{\text{bul}}$ , although with considerable intrinsic scatter (rms  $\sim 0.5$  in  $\log M_{\text{BH}}$ ; Kormendy & Richstone 1995). However,  $M_{\text{BH}}$  and the bulge effective stellar velocity dispersion  $\sigma_e$  correlate more tightly (rms  $\sim 0.3$ ) than  $M_{\text{BH}}-L_{B, \text{bul}}$  (Ferrarese & Merritt 2000; Gebhardt et al. 2000a). The smaller scatter of the  $M_{\text{BH}}-\sigma_e$  correlation suggests that the bulge dynamics (or mass), rather than luminosity, is the agent of the correlation. But the smaller spread relative to  $M_{\text{BH}}-L_{B, \text{bul}}$  appears to be an artifact of the manipulations necessary to derive  $L_{\text{bul}}$ . Indeed, recent work has shown that when bulge parameters are measured with more accuracy (e.g., profile fitting rather than an average correction for disk light; Simien & de Vaucouleurs 1986), the resulting scatter is comparable to that of  $M_{\text{BH}}-\sigma_e$  (McLure & Dunlop 2002; Erwin, Graham, & Caon 2003). The correlation between  $M_{\text{BH}}$  and bulge light concentration also has a comparably low scatter (Graham et al. 2001). Nevertheless, there are strong indications that  $L_{B, \text{bul}}$  of the brightest elliptical galaxies, for which decomposition issues are unimportant, deviate significantly from the  $M_{\text{BH}}-L_{\text{bul}}$  relation (Ferrarese 2002). Hence, longer wavelengths may also be necessary to better define the intrinsic scatter in  $M_{\text{BH}}-L_{\text{bul}}$  compared with that of  $M_{\text{BH}}-\sigma_e$ .

In this Letter, we reexamine the  $M_{\text{BH}}-L_{\text{bul}}$  correlation by accurately measuring the bulge luminosity in the near-infrared (NIR) for all galaxies with a well-determined  $M_{\text{BH}}$ . All previous studies have used optical light ( $B$  or  $R$ ) to test the  $M_{\text{BH}}-L_{\text{bul}}$  relation, but NIR light provides a clear advantage over the optical: it is a better tracer of stellar mass and less subject to the effects of extinction. If the physical correlation is between the

BH mass and the bulge mass, the NIR correlations  $M_{\text{BH}}-L_{\text{bul}}$  should be tighter than those in the optical because of the smaller variation of the  $M/L$  ratio  $\Upsilon$  with mass (e.g., Gavazzi 1993). Moreover, we use a two-dimensional bulge/disk decomposition to determine bulge parameters, an improvement on earlier work that applied one-dimensional fits only. Here we construct the largest possible sample, by considering all galaxies that have been used for the  $M_{\text{BH}}-\sigma_e$  and  $M_{\text{BH}}-L_{B, \text{bul}}$  correlations. In § 2 we present the sample of galaxies with direct dynamical BH mass measurements, and in § 3 we describe the images and the two-dimensional bulge/disk decomposition applied to them. Finally, in § 4 we discuss the results of the analysis.

### 2. THE SAMPLE

To date, there are 37 galaxies with a direct gas kinematical or stellar dynamical determination of the central BH mass. These galaxies have been compiled and made into a uniform sample (e.g., for distances) by a number of authors (e.g., Merritt & Ferrarese 2001b; Tremaine et al. 2002, hereafter T02). We adopt the data from the recent paper by T02 with some modifications and additions. The data in columns (1)–(5) and (9) of Table 1 are from the compilation by T02, and the reader can refer to that paper for more details. Differently from T02, when galaxy distances from surface brightness fluctuations (Tonry et al. 2000) are not available, we use recession velocities corrected for Virgocentric infall from the Lyon/Meudon Extragalactic Database (LEDA)<sup>3</sup> with  $H_0 = 70 \text{ km s}^{-1} \text{ Mpc}^{-1}$ . In a few cases, we also consider BH mass estimates from different papers than those used by T02; thus, in column (6), we indicate the appropriate references. With respect to the 31 galaxies considered by T02, we add Cygnus A (Tadhunter et al. 2003), M81 (Devereux et al. 2003), M84 (Bower et al. 1998), NGC 4594 (Kormendy 1988), Centaurus A (Marconi et al. 2001), and NGC 5252 (A. Capetti, D. Macchetto, D. J. Axon, & A. Marconi 2003, in preparation).

Following Merritt & Ferrarese (2001b), we divide the galaxies into two groups. In the first group, we place all the galaxies that have a secure BH mass measurement and an accurate determination of the bulge NIR luminosity. We consider “secure” those BH masses for which the BH sphere of influence,

<sup>1</sup> INAF–Osservatorio Astrofisico di Arcetri, Largo Enrico Fermi 5, I-50125 Firenze, Italy; marconi@arcetri.astro.it.

<sup>2</sup> Istituto di Radioastronomia, Sezione di Firenze/CNR, Largo Enrico Fermi 5, I-50125 Firenze, Italy; hunt@arcetri.astro.it.

<sup>3</sup> See <http://leda.univ-lyon1.fr>.

TABLE 1  
GALAXY SAMPLE

Galaxy (1)	Type (2)	$D$ (3)	$\sigma_e$ (4)	$M_{\text{BH}} (+, -)$ (5)	Ref. (6)	$R_{\text{BH}}$ (7)	$N_{\text{res}}$ (8)	$M_B$ (9)	$M_J$ (10)	$M_H$ (11)	$M_K$ (12)	$R_e$ (13)	$M_{\text{bul}}$ (14)
Group 1													
NGC 4258	Sbc	7.2	130	$3.9 (0.1, 0.1) \times 10^7$	m-1	0.28	71	-17.2	-20.9	-22.0	-22.4	$0.92 \pm 0.23$	$(1.1 \pm 0.3) \times 10^{10}$
M87	E0	16.1	375	$3.4 (1.0, 1.0) \times 10^9$	g-2	1.33	33	-21.5	-24.6	-25.2	-25.6	$6.4 \pm 1.6$	$(6.2 \pm 1.7) \times 10^{11}$
NGC 3115	S0	9.7	230	$9.1 (9.9, 2.8) \times 10^8$	s-3	1.57	15	-20.2	-23.5	-24.2	-24.4	$4.7 \pm 1.2$	$(1.7 \pm 0.5) \times 10^{11}$
NGC 4649	E1	16.8	385	$2.0 (0.4, 0.6) \times 10^9$	s-4	0.71	14	-21.3	-24.9	-25.5	-25.8	$8.1 \pm 2.0$	$(8.4 \pm 2.2) \times 10^{11}$
M81	Sb	3.9	165	$7.6 (2.2, 1.1) \times 10^7$	g-5	0.63	13	-18.2	-23.1	-23.9	-24.1	$3.4 \pm 0.9$	$(6.4 \pm 1.8) \times 10^{10}$
M84	E1	18.4	296	$1.0 (2.0, 0.6) \times 10^9$	g-6	0.55	11	-21.4	-24.7	-25.8	-25.7	$8.2 \pm 2.1$	$(5.0 \pm 1.4) \times 10^{11}$
M32	E2	0.8	75	$2.5 (0.5, 0.5) \times 10^6$	s-7	0.49	9.7	-15.8	-18.9	-19.7	-19.8	$0.24 \pm 0.06$	$(9.6 \pm 2.6) \times 10^8$
Cen A	S0	4.2	150	$2.4 (3.6, 1.7) \times 10^8$	g-8	2.25	9.0	-20.8	-23.8	-24.3	-24.5	$3.6 \pm 0.9$	$(5.6 \pm 1.5) \times 10^{10}$
NGC 4697	E4	11.7	177	$1.7 (0.2, 0.1) \times 10^8$	s-4	0.41	8.2	-20.2	-23.9	-24.5	-24.6	$9.1 \pm 2.3$	$(2.0 \pm 0.5) \times 10^{11}$
IC 1459	E3	29.2	340	$1.5 (1.0, 1.0) \times 10^9$	s-9	0.39	7.8	-21.4	-24.8	-25.3	-25.9	$8.2 \pm 2.0$	$(6.6 \pm 1.8) \times 10^{11}$
NGC 5252	S0	96.8	190	$1.0 (0.2, 0.4) \times 10^9$	g-10	0.25	5.1	-20.8	-24.4	-25.2	-25.6	$9.7 \pm 2.4$	$(2.4 \pm 0.9) \times 10^{11}$
NGC 2787	SB0	7.5	140	$4.1 (0.4, 0.5) \times 10^7$	g-11	0.25	5.0	-17.3	-20.4	-21.1	-21.3	$0.32 \pm 0.08$	$(4.4 \pm 1.2) \times 10^9$
NGC 4594	Sa	9.8	240	$1.0 (1.0, 0.7) \times 10^9$	s-12	1.57	5.0	-21.3	-24.2	-24.8	-25.4	$5.1 \pm 1.3$	$(2.0 \pm 0.5) \times 10^{11}$
NGC 3608	E2	22.9	182	$1.9 (1.0, 0.6) \times 10^8$	s-4	0.22	4.4	-19.9	-23.4	-24.0	-24.1	$4.3 \pm 1.1$	$(9.9 \pm 2.7) \times 10^{10}$
NGC 3245	S0	20.9	205	$2.1 (0.5, 0.5) \times 10^8$	g-13	0.21	4.2	-19.6	-22.4	-23.1	-23.3	$1.3 \pm 0.3$	$(3.9 \pm 1.0) \times 10^{10}$
NGC 4291	E2	26.2	242	$3.1 (0.8, 2.3) \times 10^8$	s-4	0.18	3.6	-19.6	-23.1	-23.8	-23.9	$2.3 \pm 0.6$	$(9.5 \pm 2.5) \times 10^{10}$
NGC 3377	E5	11.2	145	$1.0 (0.9, 0.1) \times 10^8$	s-4	0.38	3.6	-19.0	-22.7	-23.5	-23.6	$5.4 \pm 1.3$	$(7.8 \pm 2.1) \times 10^{10}$
NGC 4473	E5	15.7	190	$1.1 (0.4, 0.8) \times 10^8$	s-4	0.17	3.4	-19.9	-23.1	-23.6	-23.8	$2.8 \pm 0.7$	$(6.9 \pm 1.9) \times 10^{10}$
Cygnus A	E	240	270	$2.9 (0.7, 0.7) \times 10^9$	g-14	0.15	2.9	-21.9	-26.4	-26.9	-27.3	$31 \pm 8$	$(1.6 \pm 1.1) \times 10^{12}$
NGC 4261	E2	31.6	315	$5.2 (1.0, 1.1) \times 10^8$	g-15	0.15	2.9	-21.1	-24.6	-25.4	-25.6	$6.5 \pm 1.6$	$(4.5 \pm 1.2) \times 10^{11}$
NGC 4564	E3	15.0	162	$5.6 (0.3, 0.8) \times 10^7$	s-4	0.13	2.5	-18.9	-22.5	-23.3	-23.4	$3.0 \pm 0.7$	$(5.4 \pm 1.5) \times 10^{10}$
NGC 4742	E4	15.5	90	$1.4 (0.4, 0.5) \times 10^7$	s-16	0.10	2.0	-18.9	-22.1	-22.8	-23.0	$2.0 \pm 0.5$	$(1.1 \pm 0.3) \times 10^{10}$
NGC 3379	E1	10.6	206	$1.0 (0.6, 0.5) \times 10^8$	s-17	0.20	1.9	-19.9	-23.1	-23.7	-24.2	$2.9 \pm 0.7$	$(8.5 \pm 2.3) \times 10^{10}$
NGC 1023	SB0	11.4	205	$4.4 (0.5, 0.5) \times 10^7$	s-18	0.08	1.6	-18.4	-22.6	-23.3	-23.5	$1.2 \pm 0.3$	$(3.4 \pm 0.9) \times 10^{10}$
NGC 5845	E3	25.9	234	$2.4 (0.4, 1.4) \times 10^8$	s-4	0.15	1.4	-18.7	-22.0	-22.7	-23.0	$0.50 \pm 0.12$	$(1.9 \pm 0.5) \times 10^{10}$
NGC 3384	S0	11.6	143	$1.6 (0.1, 0.2) \times 10^7$	s-4	0.06	1.2	-19.0	-21.7	-22.3	-22.6	$0.49 \pm 0.12$	$(7.0 \pm 1.9) \times 10^9$
NGC 6251	E2	107.0	290	$6.1 (2.0, 2.1) \times 10^8$	g-19	0.06	1.2	-21.5	-25.4	-26.4	-26.6	$11 \pm 3$	$(6.7 \pm 1.8) \times 10^{11}$
Group 2 <sup>a</sup>													
Milky Way	SBbc	0.008	103	$4.1 (0.6, 0.6) \times 10^6$	s-20	42.9	1714	-17.6	-22.0	-22.2	-22.3	$0.70 \pm 0.20$	$(5.2 \pm 2.5) \times 10^9$
M31	Sb	0.8	160	$4.5 (4.0, 2.5) \times 10^7$	s-21	2.05	41	-19.0	-21.8	-22.5	-22.8	$1.0 \pm 0.3$	$(1.9 \pm 0.5) \times 10^{10}$
NGC 1068	Sb	15.0	151	$8.3 (0.3, 0.3) \times 10^6$	m-22	0.02	2.7	-18.8	-23.6	-24.7	-25.0	$3.1 \pm 0.8$	$(5.0 \pm 1.4) \times 10^{10}$
NGC 4459	S0	16.1	186	$7.0 (1.3, 1.3) \times 10^7$	g-11	0.11	2.2	-19.1	-23.9	-24.2	-24.5	$15 \pm 4$	$(3.6 \pm 1.0) \times 10^{11}$
NGC 4596	SB0	27.9	152	$7.8 (4.2, 3.3) \times 10^7$	g-11	0.11	2.1	-20.6	-23.0	-23.7	-23.8	$1.6 \pm 0.4$	$(2.6 \pm 0.7) \times 10^{10}$
NGC 7457	S0	13.2	67	$3.5 (1.1, 1.4) \times 10^6$	s-4	0.05	1.0	-17.7	-21.3	-22.0	-21.8	$4.8 \pm 3.5$	$(1.5 \pm 1.1) \times 10^{10}$
NGC 4342	S0	11.4	225	$2.2 (1.3, 0.8) \times 10^8$	s-23	0.34	0.8	-16.4	-20.1	-20.7	-20.7	$0.29 \pm 0.07$	$(1.0 \pm 0.3) \times 10^{10}$
NGC 0821	E4	24.1	209	$3.7 (2.4, 0.8) \times 10^7$	s-4	0.03	0.6	-20.4	-24.4	-24.9	-24.8	$20 \pm 5$	$(6.2 \pm 1.7) \times 10^{11}$
NGC 2778	E2	22.9	175	$1.4 (0.8, 0.9) \times 10^7$	s-4	0.02	0.4	-18.6	-22.0	-22.8	-23.0	$3.0 \pm 0.8$	$(6.5 \pm 1.7) \times 10^{10}$
NGC 7052	E4	71.4	266	$4.0 (2.8, 1.6) \times 10^8$	g-24	0.07	0.5	-21.7	-25.2	-25.9	-26.1	$12 \pm 3$	$(6.0 \pm 1.6) \times 10^{11}$

COLUMNS.—(1) Galaxy name. (2) Morphological type from de Vaucouleurs et al. 1991. (3) Galaxy distance in megaparsecs. (4) Stellar velocity dispersions from T02 and Kormendy & Gebhardt 2001 in units of kilometers per second. All  $\sigma_e$ -values have  $\pm 5\%$  errors except for the Milky Way ( $\pm 20$  km s<sup>-1</sup>), Cygnus A ( $\pm 90$  km s<sup>-1</sup>; Thornton, Stockton, & Ridgway 1999), and NGC 5252 ( $\pm 27$  km s<sup>-1</sup>). (5) BH mass in units of solar mass. The plus, minus signs indicate the plus and minus errors. (6) Method of  $M_{\text{BH}}$  determination (g = gas kinematics, s = stellar dynamics, m = gas kinematics with maser spots) and references from where  $M_{\text{BH}}$  was obtained (if necessary, it was rescaled to the distances in col. [3]). (7) BH sphere of influence,  $R_{\text{BH}} = GM_{\text{BH}}/\sigma_e^2$ , in arcseconds. (8)  $N_{\text{res}} = 2R_{\text{BH}}/R_{\text{res}}$ , where  $R_{\text{res}}$  is the spatial resolution of the observations. (9) Absolute bulge  $B$  luminosity from T02 or extracted from the Third Reference Catalogue of Bright Galaxies (de Vaucouleurs et al. 1991). (10)–(12) Absolute  $J$ ,  $H$ , and  $K$  bulge magnitudes. Milky Way  $J$ - and  $K$ -values are taken from Dwek et al. 1995, while for M31 we have corrected the total galaxy magnitudes (Malhotra et al. 1996) with the Simien & de Vaucouleurs 1986 disk/bulge average ratios;  $H$ -values are interpolated. All  $M_J$ ,  $M_H$ , and  $M_K$ -values have errors  $\pm 0.1$  mag except for the Milky Way ( $\Delta M_J = 0.75$ ,  $\Delta M_H = 0.75$ ,  $\Delta M_K = 0.75$ ), M31 (0.4, 0.5, 0.4), Centaurus A (0.2, 0.3, 0.2), NGC 1068 (0.6, 0.6, 0.6), and NGC 7457 (0.6, 0.4, 0.4). (13)  $J$ -band effective bulge radius in kiloparsecs. For the Milky Way, we have taken the estimate of T02, while for M31 we have used that of Kormendy & Bender 1999. (14) Virial bulge mass in units of solar mass.

REFERENCES.—(1) Herrnstein et al. 1999; (2) Macchetto et al. 1997; (3) Emsellem, Dejonghe, & Bacon 1999; (4) Gebhardt et al. 2003; (5) Devereux et al. 2003; (6) average of Bower et al. 1998 and Maciejewski & Binney 2001; (7) Verolme et al. 2002; (8) Marconi et al. 2001; (9) average of Verdoes Kleijn et al. 2000 and Cappellari et al. 2002; (10) A. Capetti, D. Macchetto, D. J. Axon, & A. Marconi 2003, in preparation; (11) Sarzi et al. 2001; (12) Kormendy 1988; (13) Barth et al. 2001; (14) Tadhunter et al. 2003; (15) Ferrarese, Ford, & Jaffe 1996; (16) T02; (17) Gebhardt et al. 2000b; (18) Bower et al. 2001; (19) Ferrarese & Ford 1999; (20) Ghez et al. 2003 and Schödel et al. 2002; (21) Tremaine 1995, Kormendy & Bender 1999, and Bacon et al. 2001; (22) Lodato & Bertin 2003 and Greenhill et al. 1996; (23) Cretton & van den Bosch 1999; (24) van der Marel & van den Bosch 1998

<sup>a</sup> Although the Milky Way represents by far the best case for a BH, it has been placed in group 2 because existing measurements of the bulge NIR luminosity are uncertain and because it is beyond the scope of this Letter to estimate the luminosity of the Milky Way bulge from 2MASS data. This is also the case for M31. NGC 1068 is in group 2 because the BH mass estimate is not “secure” in the sense that the maser spots are moving in a sub-Keplerian manner (Greenhill et al. 1996), and  $M_{\text{BH}}$  depends on the adopted disk model (Lodato & Bertin 2003). Also, the complex morphology did not allow us to obtain an accurate estimate of the bulge luminosity. In the cases of NGC 4459 and NGC 4596, the data do not allow a tight constraint on  $M_{\text{BH}}$  (Sarzi et al. 2001).

$R_{\text{BH}} = GM_{\text{BH}}/\sigma_e^2$  (col. [7] of Table 1), has been clearly resolved, i.e.,  $N_{\text{res}} = 2R_{\text{BH}}/R_{\text{res}} > 1$ , where  $R_{\text{res}}$  is the spatial resolution of the observations. Additional reasons for placing galaxies in group 2 are given in Table 1.

### 3. IMAGE ANALYSIS

We have constructed a homogeneous set of NIR images of the galaxies presented in Table 1 (except for the Milky Way

and M31) by retrieving  $J$ ,  $H$ , and  $K$  atlas images from the Two Micron All Sky Survey (2MASS).<sup>4</sup> When a single atlas image contained only a portion of the galaxy, we also retrieved adjacent tiles and mosaicked the images after subtracting the sky background and rescaling for the different zero points. The

<sup>4</sup> See <http://www.ipac.caltech.edu/2mass>.

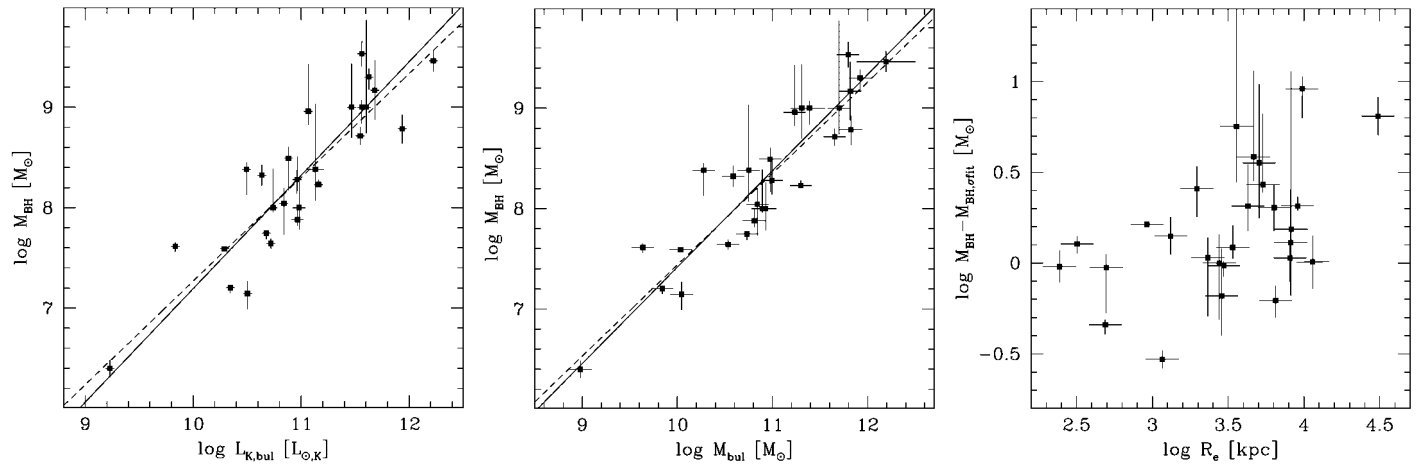


FIG. 1.—*Left*:  $M_{\text{BH}}$  vs.  $L_{K,\text{bul}}$  for the galaxies of group 1. The solid lines are obtained with the bisector linear regression algorithm of Akritas & Bershady (1996), while the dashed lines are ordinary least-squares fits. *Middle*:  $M_{\text{BH}}$  vs.  $M_{\text{bul}}$  with the same notation as in the previous panel. *Right*: Residuals of  $M_{\text{BH}} - \sigma_e$  vs.  $R_e$ , in which we use the  $M_{\text{BH}} - \sigma_e$  regression of T02.

2MASS images are photometrically calibrated with a typical accuracy of a few percent. More details can be found in L. K. Hunt & A. Marconi (2003, in preparation, hereafter Paper II).

We performed a two-dimensional bulge/disk decomposition of the images using the program GALFIT (Peng et al. 2002), which is made publicly available by the authors. This code allows the fitting of several components with different functional shapes (e.g., generalized exponential [Sersic] and simple exponential laws); the best-fit parameters are determined by minimizing  $\chi^2$ . More details on GALFIT can be found in Peng et al. (2002). We fitted separately the  $J$ ,  $H$ , and  $K$  images. Each fit was started by fitting a single Sersic component and constant background. When necessary (e.g., for spiral galaxies), an additional component (usually an exponential disk) was added. In many cases, these initial fits left large residuals, and we thus increased the number of components (see also Peng et al. 2002). The fits are described in detail in Paper II. In Table 1, we present the  $J$ ,  $H$ , and  $K$  bulge magnitudes, effective bulge radii  $R_e$  in the  $J$  band, and their uncertainties. The  $J$ ,  $H$ , and  $K$  magnitudes were corrected for Galactic extinction using the data of Schlegel, Finkbeiner, & Davis (1998). We used the  $J$  band to determine  $R_e$  because the images tend to be flatter, and thus the background is better determined.

#### 4. RESULTS AND DISCUSSION

In Figure 1, we plot, from left to right,  $M_{\text{BH}}$  versus  $L_{K,\text{bul}}$ ,  $M_{\text{BH}}$  versus  $M_{\text{bul}}$ , and the residuals of  $M_{\text{BH}} - \sigma_e$  versus  $R_e$  (based on the fit from T02). Only group 1 galaxies are shown.  $M_{\text{bul}}$  is the virial bulge mass given by  $kR_e\sigma_e^2/G$ ; if bulges behave as isothermal spheres,  $k = 8/3$ . However, comparing our virial estimates of  $M_{\text{bul}}$  with those of  $M_{\text{dyn}}$ , obtained from dynamical modeling (Magorrian et al. 1998; Gebhardt et al. 2003), shows that  $M_{\text{bul}}$  and  $M_{\text{dyn}}$  are well correlated ( $r = 0.88$ ); setting

$k = 3$  (rather than  $8/3$ ) gives an average ratio of unity. Therefore, we have used  $k = 3$  in the above formula. Considering the uncertainties of both mass estimates, the scatter of the ratio  $M_{\text{bul}}/M_{\text{dyn}}$  is 0.21 dex. We fitted the data with the bisector linear regression from Akritas & Bershady (1996) that allows for uncertainties on both variables and intrinsic dispersion. The FITEXY routine (Press et al. 1992) used by T02 gives consistent results (see Fig. 1). Fit results of  $M_{\text{BH}}$  versus the galaxy properties for group 1 and the combined samples are summarized in Table 2. The intrinsic dispersion of the residuals (rms) has been estimated with a maximum likelihood method assuming normally distributed values. Inspection of Figure 1 and Table 2 shows that  $L_{K,\text{bul}}$  and  $M_{\text{bul}}$  correlate well with the BH mass. The correlation between  $M_{\text{BH}}$  and  $M_{\text{bul}}$  is equivalent to that between the radius of the BH sphere of influence  $R_{\text{BH}} (= GM_{\text{BH}}/\sigma_e^2)$  and  $R_e$ .

##### 4.1. Intrinsic Dispersion of the Correlations

To compare the scatter of  $M_{\text{BH}} - L_{\text{bul}}$  for different wave bands, we have also analyzed the  $B$ -band bulge luminosities for our sample. The upper limit of the intrinsic dispersion of the  $M_{\text{BH}} - L_{\text{bul}}$  correlations goes from  $\sim 0.5$  dex in  $\log M_{\text{BH}}$  when considering all galaxies to  $\sim 0.3$  dex when considering only those of group 1. Hence, for galaxies with reliable  $M_{\text{BH}}$  and  $L_{\text{bul}}$ , the scatter of  $M_{\text{BH}} - L_{\text{bul}}$  correlations is  $\sim 0.3$  dex, *independently of the spectral band used (B or JHK)*, comparable to that of  $M_{\text{BH}} - \sigma_e$ . This scatter would be smaller if the measurement errors are underestimated. McLure & Dunlop (2002) and Erwin et al. (2003) reached a similar conclusion using  $R$ -band  $L_{\text{bul}}$ , but on smaller samples. The correlation between the  $R$ -band bulge light concentration and  $M_{\text{BH}}$  has a comparable scatter (Graham et al. 2001).

Since  $M_{\text{BH}} - L_{B,\text{bul}}$  and  $M_{\text{BH}} - L_{\text{NIR,bul}}$  have comparable disper-

TABLE 2  
FIT RESULTS ( $\log M_{\text{BH}} = a + bX$ )

$X$	GROUP 1 GALAXIES			ALL GALAXIES		
	$a$	$b$	rms	$a$	$b$	rms
$\log L_{B,\text{bul}} - 10.0$ .....	$8.18 \pm 0.08$	$1.19 \pm 0.12$	0.32	$8.07 \pm 0.09$	$1.26 \pm 0.13$	0.48
$\log L_{J,\text{bul}} - 10.7$ .....	$8.26 \pm 0.07$	$1.14 \pm 0.12$	0.33	$8.10 \pm 0.10$	$1.24 \pm 0.15$	0.53
$\log L_{H,\text{bul}} - 10.8$ .....	$8.19 \pm 0.07$	$1.16 \pm 0.12$	0.33	$8.04 \pm 0.10$	$1.25 \pm 0.15$	0.52
$\log L_{K,\text{bul}} - 10.9$ .....	$8.21 \pm 0.07$	$1.13 \pm 0.12$	0.31	$8.08 \pm 0.10$	$1.21 \pm 0.13$	0.51
$\log M_{\text{bul}} - 10.9$ .....	$8.28 \pm 0.06$	$0.96 \pm 0.07$	0.25	$8.12 \pm 0.09$	$1.06 \pm 0.10$	0.49

sions, the rough bulge/disk decomposition (§ 1), the larger reddening, and stellar population effects do not apparently compromise the correlation. Most of the galaxies in the sample are early types and thus may be less sensitive to the above effects. However, the scatter in the  $M_{\text{BH}}-L_{\text{bul}}$  correlations does not decrease significantly when considering only elliptical galaxies.

The correlation between  $M_{\text{BH}}$  and  $M_{\text{bul}}$  has a slightly lower dispersion (0.25 dex vs. 0.3 dex) than  $M_{\text{BH}}-L_{\text{bul}}$ . If the scatter of  $M_{\text{bul}}-M_{\text{dyn}}$  (0.21 dex) is an indication of the additional uncertainties on our virial estimates, then the intrinsic scatter of  $M_{\text{BH}}-M_{\text{bul}}$  drops to  $\sim 0.15$  dex. Judging from the present data, in which only secure  $M_{\text{BH}}$  and  $L_{\text{bul}}$  are included,  $\sigma_e$ ,  $M_{\text{bul}}$ ,  $L_{B, \text{bul}}$ , and  $L_{\text{NIR, bul}}$  provide equally good  $M_{\text{BH}}$  estimates to within a factor of  $\sim 2$ .

#### 4.2. Correlation Slopes

All the slopes are roughly unity, but those of  $M_{\text{BH}}-L_{\text{bul}}$  are systematically larger than that of  $M_{\text{BH}}-M_{\text{bul}}$ . This is expected if  $L_{\text{bul}}$  correlates with  $M_{\text{BH}}$  because of its dependence on  $M_{\text{bul}}$  through the stellar  $M/L$  ratio. From our  $M_{\text{bul}}-L_{\text{bul}}$  relation, we find that  $\log \Upsilon_K = 0.18 \log L_{K, \text{bul}} - 2.1$ ; the weak dependence of  $\Upsilon$  on  $L$  fully accounts for the different slopes of  $M_{\text{BH}}-L_{K, \text{bul}}$  and  $M_{\text{BH}}-M_{\text{bul}}$ . The same applies to the  $J$  and  $H$  bands.

All correlations are thus consistent with a direct proportionality between  $M_{\text{BH}}$  and bulge mass. This contrasts with previous claims of a nonlinearity of the  $M_{\text{BH}}-M_{\text{bul}}$  relation (Laor 2001) but is in agreement with McLure & Dunlop (2002). A partial correlation analysis of  $\log M_{\text{BH}}$  (variable  $x_1$ ),  $\log \sigma_e$  ( $x_2$ ), and  $\log R_e$  ( $x_3$ ) shows that  $M_{\text{BH}}$  is *separately* significantly correlated both with  $\sigma_e$  and with  $R_e$ . The Pearson partial correlation co-

efficients, in which the known dependence of  $\sigma_e$  and  $R_e$  is eliminated, are  $r_{12} = 0.83$  and  $r_{13} = 0.65$ , with a significance of greater than 99.9%. This is shown graphically in the right-most panel of Figure 1, where the residuals of the T02  $M_{\text{BH}}-\sigma_e$  correlation are plotted against  $R_e$ ; there is a weak, but significant, correlation of these residuals with  $R_e$ . Consequently, when galaxy structural parameters are measured carefully from a two-dimensional image analysis, the additional, weaker, dependence of  $M_{\text{BH}}$  on  $R_e$  is uncovered. Thus, a combination of both  $\sigma_e$  and  $R_e$  is necessary to drive the correlations between  $M_{\text{BH}}$  and other bulge properties. This *fundamental plane* of BHs will be further investigated elsewhere.

The average  $\log (M_{\text{BH}}/M_{\text{bul}})$  can be estimated assuming a log-normal distribution with normally distributed observational errors. With maximum likelihood, we find  $\langle \log (M_{\text{BH}}/M_{\text{bul}}) \rangle = -2.63$  with an intrinsic dispersion of 0.27 dex ( $-2.79$  and  $0.49$  dex for all galaxies). Adopting the method of Merritt & Ferrarese (2001a), we find  $\langle \log (M_{\text{BH}}/M_{\text{bul}}) \rangle = -2.81$  and rms =  $0.36$  ( $-2.86$  and  $0.44$  dex for all galaxies), consistent with their result of  $-2.9$  and  $0.45$  dex (see also McLure & Dunlop 2002).

We thank A. Capetti, E. Emsellem, W. Maciejewski, C. Norman, and E. Oliva for useful discussions and C. Peng for making GALFIT publicly available. This Letter was partially supported by ASI (I/R/112/01 and I/R/048/02) and MIUR (Cofin 01-02-02). This publication uses the LEDA database, NED, the NASA/IPAC Extragalactic Database operated by JPL, Caltech, under contract with NASA, and data products from 2MASS, a joint project of the University of Massachusetts and the IPAC/Caltech, funded by NASA and NSF.

#### REFERENCES

- Akritas, M. G., & Bershady, M. A. 1996, *ApJ*, 470, 706  
 Aller, M. C., & Richstone, D. 2002, *AJ*, 124, 3035  
 Bacon, R., Emsellem, E., Combes, F., Copin, Y., Monnet, G., & Martin, P. 2001, *A&A*, 371, 409  
 Barth, A. J., Sarzi, M., Rix, H.-W., Ho, L. C., Filippenko, A. V., & Sargent, W. L. W. 2001, *ApJ*, 555, 685  
 Bower, G. A., et al. 2001, *ApJ*, 550, 75  
 ———. 1998, *ApJ*, 492, L111  
 Cappellari, M., et al. 2002, *ApJ*, 578, 787  
 Cretton, N., & van den Bosch, F. C. 1999, *ApJ*, 514, 704  
 de Vaucouleurs, G., de Vaucouleurs, A., Corwin, H. G., Jr., Buta, R. J., Pasturel, G., & Fouqué, P. 1991, *Third Reference Catalogue of Bright Galaxies* (New York: Springer)  
 Devereux, N. A., Ford, H. C., Tsvetanov, Z., & Jacoby, G. 2003, *AJ*, 125, 1226  
 Dwek, E., et al. 1995, *ApJ*, 445, 716  
 Emsellem, E., Dejonghe, H., & Bacon, R. 1999, *MNRAS*, 303, 495  
 Erwin, P., Graham, A. W., & Caon, N. 2003, in *Coevolution of Black Holes and Galaxies*, ed. L. C. Ho (Carnegie Obs. Astrophys. Ser., Vol. 1; Pasadena: Carnegie Obs.), in press (astro-ph/0212335)  
 Ferrarese, L. 2002, in *Current High-Energy Emission around Black Holes*, eds. C.-H. Lee & H.-Y. Chang (Singapore: World Scientific), 3  
 Ferrarese, L., & Ford, H. C. 1999, *ApJ*, 515, 583  
 Ferrarese, L., Ford, H. C., & Jaffe, W. 1996, *ApJ*, 470, 444  
 Ferrarese, L., & Merritt, D. 2000, *ApJ*, 539, L9  
 Gavazzi, G. 1993, *ApJ*, 419, 469  
 Gebhardt, K., et al. 2000a, *ApJ*, 539, L13  
 ———. 2000b, *AJ*, 119, 1157  
 ———. 2003, *ApJ*, 583, 92  
 Ghez, A. M., et al. 2003, *ApJ*, 586, L127  
 Graham, A. W., Erwin, P., Caon, N., & Trujillo, I. 2001, *ApJ*, 563, L11  
 Greenhill, L. J., Gwinn, C. R., Antonucci, R., & Barvainis, R. 1996, *ApJ*, 472, L21  
 Herrnstein, J. R., et al. 1999, *Nature*, 400, 539  
 Kormendy, J. 1988, *ApJ*, 335, 40  
 Kormendy, J., & Bender, R. 1999, *ApJ*, 522, 772  
 Kormendy, J., & Gebhardt, K. 2001, in *AIP Conf. Proc. 586, 20th Texas Symp. on Relativistic Astrophysics*, ed. J. C. Wheeler & H. Martel (Melville: AIP), 363  
 Kormendy, J., & Richstone, D. 1995, *ARA&A*, 33, 581  
 Laor, A. 2001, *ApJ*, 553, 677  
 Lodato, G., & Bertin, G. 2003, *A&A*, 398, 517  
 Macchetto, F., Marconi, A., Axon, D. J., Capetti, A., Sparks, W., & Crane, P. 1997, *ApJ*, 489, 579  
 Maciejewski, W., & Binney, J. 2001, *MNRAS*, 323, 831  
 Magorrian, J., et al. 1998, *AJ*, 115, 2285  
 Malhotra, S., Spergel, D. N., Rhoads, J. E., & Li, J. 1996, *ApJ*, 473, 687  
 Marconi, A., Capetti, A., Axon, D. J., Koekemoer, A., Macchetto, D., & Schreier, E. J. 2001, *ApJ*, 549, 915  
 Marconi, A., & Salvati, M. 2002, in *ASP Conf. Ser. 258, Issues in Unification of Active Galactic Nuclei*, ed. R. Maiolino, A. Marconi, & N. Nagar (San Francisco: ASP), 217  
 McLure, R. J., & Dunlop, J. S. 2002, *MNRAS*, 331, 795  
 Merritt, D., & Ferrarese, L. 2001a, *MNRAS*, 320, L30  
 ———. 2001b, in *ASP Conf. Ser. 249, The Central Kiloparsec of Starbursts and AGN*, ed. J. H. Knapen, J. E. Beckman, I. Shlosman, & T. J. Mahoney (San Francisco: ASP), 335  
 Peng, C. Y., Ho, L. C., Impey, C. D., & Rix, H.-W. 2002, *AJ*, 124, 266  
 Press, W. H., et al. 1992, *Numerical Recipes in C* (2d ed.; Cambridge: Cambridge Univ. Press)  
 Sarzi, M., Rix, H.-W., Shields, J. C., Rudnick, G., Ho, L. C., McIntosh, D. H., Filippenko, A. V., & Sargent, W. L. W. 2001, *ApJ*, 550, 65  
 Schlegel, D. J., Finkbeiner, D. P., & Davis, M. 1998, *ApJ*, 500, 525  
 Schödel, R., et al. 2002, *Nature*, 419, 694  
 Simien, F., & de Vaucouleurs, G. 1986, *ApJ*, 302, 564  
 Sołtan, A. 1982, *MNRAS*, 200, 115  
 Tadhunter, C., Marconi, A., Axon, D., Wills, K., Robinson, T. G., & Jackson, N. 2003, *MNRAS*, in press (astro-ph/0302513)  
 Thornton, R. J., Stockton, A., & Ridgway, S. E. 1999, *AJ*, 118, 1461  
 Tonry, J., Blakeslee, J., Ajhar, E., & Dressler, A. 2000, *ApJ*, 530, 625  
 Tremaine, S. 1995, *AJ*, 110, 628  
 Tremaine, S., et al. 2002, *ApJ*, 574, 740 (T02)  
 van der Marel, R. P., & van den Bosch, F. C. 1998, *AJ*, 116, 2220  
 Verdoes Kleijn, G. A., van der Marel, R. P., Carollo, C. M., & de Zeeuw, P. T. 2000, *AJ*, 120, 1221  
 Verolme, E. K., et al. 2002, *MNRAS*, 335, 517  
 Yu, Q., & Tremaine, S. 2002, *MNRAS*, 335, 965